Polymer Degradation and Stability 98 (2013) 1780–1783

Contents lists available at SciVerse ScienceDirect

Polymer Degradation and Stability

journal homepage: www.elsevier.com/locate/polydegstab

The discovery of free radicals in ancient silk textiles

Decai Gong*, Haiyan Yang

Basic Research Center of Conservation Science, Department of the History of Science and Scientific Archaeology, School of Humanities & Social Sciences, University of Science and Technology of China, Hefei 230026, PR China

ARTICLE INFO

Article history:
Received 10 March 2013
Received in revised form
30 April 2013
Accepted 20 May 2013
Available online 28 May 2013

Keywords:
Ancient silk textiles
Raman spectroscopy
EPR spectroscopy
Carbon radicals

ABSTRACT

Protection of ancient silk textiles from further deterioration is of vital importance to the investigation and preservation of ancient Chinese culture. Ancient silk textiles from several different ages (more than 2000 years ago) and regions were studied by means of Raman and electron paramagnetic resonance (EPR) spectroscopy in an attempt to unveil the deterioration mechanism of silk. The Raman spectra showed two peaks (***D*** and ***G***), which are indicative of carbonization. The EPR spectra of the ancient samples showed a characteristic sharp absorption centered at g ~ 2.0037 without a hyperfine structure, and have been identified as those of carbon radicals. These free radicals had not been discovered in ancient silk fabrics before, and the discovery may shed light on the deterioration mechanisms of ancient silk textiles.

1. Introduction

Silks, the major trade along the known "Silk Road", have written a magnificent page in the history of ancient Chinese civilization. However, only a small amount of ancient silks have survived after a long burial period, suffering from discoloration, low strength, *etc.* Therefore, it is of urgency to prevent these invaluable relics from further deteriorating.

Raw silk is composed of silk fibroin and sericin, two types of proteins consisting of C, H, O, N, S, *etc.* secreted by the silkworm. The role of sericin is mainly to envelop the fibroin, providing protections to the latter [1–3]. Silk textiles, however, are generally made of silks that have undergone a degumming process in which most of the sericin has been removed. As a result, silk textiles are damageable since fibroin is susceptible to different ambient factors, *e.g.* light, heat, water, and microorganisms [4,5]. In the literature, the artificial degradation behaviors induced by these factors are investigated in series. For example, amino acids in fibroin, such as glycine, alanine, tyrosine and serine, were photo-oxidized under UV-irradiation, resulting in α-ketoacyl groups [6]; silk fibers were carbonized and became amorphous when exposed to 570 K heating treatment while fibroin heavy chain (FibH, 350 kDa) and fibroin light chain (FibL, 26 kDa) started to degrade at ~350 K and ~400 K, respectively [7]; in the enzymatic degradation process, β-sheet silk crystals were first degraded into nanofibrils and finally nanofilaments and soluble silk fragments [8]. This enzymatic degradation mechanism was related to the hydrophilic interaction and crystal-noncrystal alternate nanostructures [9]. These aforementioned experiments were performed artificially on the modern silk textiles with respect to a single factor, which is hardly to simulate the complicate process of deterioration of ancient silk textiles under the natural burial environments. Thus, investigating the deterioration of ancient silks is quite meaningful to the conservation of such textile heritages. To date, various methods, *e.g.* the diluted solution viscometry [4,5], amino acid analysis [4,10,11], scanning electron microscope (SEM) [12,13], Fourier Transform infrared spectroscopy (FT-IR) [13–16] and X-ray diffraction (XRD) [17,18], *etc.*, have been utilized in the characterization of silk degradation at the holistic level. In addition, electron paramagnetic resonance (EPR) spectroscopy, a non-destructive method to detect the presence of the unpaired electron(s), can be employed to investigate the deterioration kinetics of proteins at the electronic and atomic level and probe the radical chemistry [19]. It has proved a powerful technique to trace the free radical(s) of artificially aged proteins caused by gamma-ray [20,21] and ultraviolet irradiation [22,23]. It was expected that EPR would also prove effective in the research on free radicals in ancient silk textiles, the species and even the existence of which had not yet been determined.

In this paper, the deterioration behaviors of three ancient silk textiles made between 403 B.C. and 9 A.D. and unearthed from different regions were studied via Raman and EPR spectroscopy using a modern silk fragment as a control. The results demonstrate that

* Corresponding author. Tel./fax: +86 551 6360 0232.
E-mail address: gdclucky@ustc.edu.cn (D. Gong).

0141-3910/$ – see front matter © 2013 Elsevier Ltd. All rights reserved.
http://dx.doi.org/10.1016/j.polymdegradstab.2013.05.011

carbon radical is taking part in the deterioration process. The data will shed light on the deterioration mechanism of ancient silk textiles and pave the way for better preserving these textile heritages.

2. Materials and methods

2.1. Ancient and modern silk textiles

The three ancient samples investigated are debris of silk textiles unearthed from Baling Mount, Jingzhou, Hubei Province, Lu'an, An'hui Province and Tianshan, Yangzhou, Jiangsu Province, denoted by Jingzhou (JZ), Lu'an "huangwei (coffin covering)" (LA) and Yangzhou (YZ), respectively. JZ and LA were traced back to the Warring States Period (403 B.C.–221 B.C.) and YZ to the Western Han Dynasty (202 B.C.–9 A.D.). Commercially available modern silk from Guanghua Silk Co. Ltd., Hefei City is used as control sample. It is worth noting that LA sample was collected from the debris of huangwei, the cover on the coffin (No. M585) with 184.5 cm in length and 88 cm in width. Such full-size huangwei from the Warring States Period is extremely rare throughout the country.

2.2. Characterization techniques

The samples were observed and pictured by KEYENCE VHX-2000C imaging optical microscope (KEYENCE Co., LTD, Japan). Raman spectroscopy analyses were performed at ambient temperature using the LABRAM-HR confocal microscopy laser Raman spectrometer (JY Co., France) equipped with a 514.5 nm argon ion laser with beam power of 1 mW. The spectra were recorded in the wavelength range of 500 cm^{-1}–2000 cm^{-1}. For EPR measurements, 10 mg of each sample was collected and placed into standard quartz EPR tubes. The EPR spectra were performed with a Japanese JEOL JES-FA200 EPR spectrometer at room temperature. The parameters were the microwave frequency of 9.06 GHz, the microwave power of 0.998 mW, and the modulation amplitude of 0.35 mT.

3. Results and discussions

3.1. The morphological comparison

Morphological differences between the four samples mentioned above were studied by the optical microscope. The fabric structure and color are shown in Fig. 1a–d. The modern control sample is a crepe de chine fabric (Fig. 1a) and the JZ silk textile has a plain-woven structure with indistinct fabric density (Fig. 1b). As shown in Fig. 1c, the structure of LA is warp backed-woven with warp thread of 95 cm^{-1} and weft thread of 56 cm^{-1}. The YZ sample, which is also a plain-woven textile, shows distinct fabric density of warp and weft thread being 120 cm^{-1} and 80 cm^{-1} (Fig. 1d), respectively. The color is one of the visual degradation characteristics of the undyed silk, which darkens with the increasing of the degree of deterioration [24,25]. As depicted in the figure, the original color of silk (modern control sample) is white, however, it changes to light brown, dark brown and then black of JZ, LA and YZ ancient silks, respectively. Furthermore, the dyes of these debris of ancient silk textiles have been investigated via liquid chromatography-mass spectrometry and no colorant was found. Thus, the darkened color indicates that the JZ silk is the least aged and the YZ is the most decayed one. Noteworthily, breakage occurred on the edge of the YZ sample (data not shown) due to its fragility while others felt more elastic upon touching. It is reasonable to speculate that the abnormal degradation degree of YZ sample (the youngest but the most deteriorated) resulted from the different burial environments since buried silks are sensitive to heat, water, microorganisms, *etc.* of the tomb.

3.2. The Raman spectroscopy analysis

It is well established that Raman spectroscopy is a powerful technique to probe the carbonization of the silk fibroin [26–28]. The Raman spectra obtained from the four samples are shown in

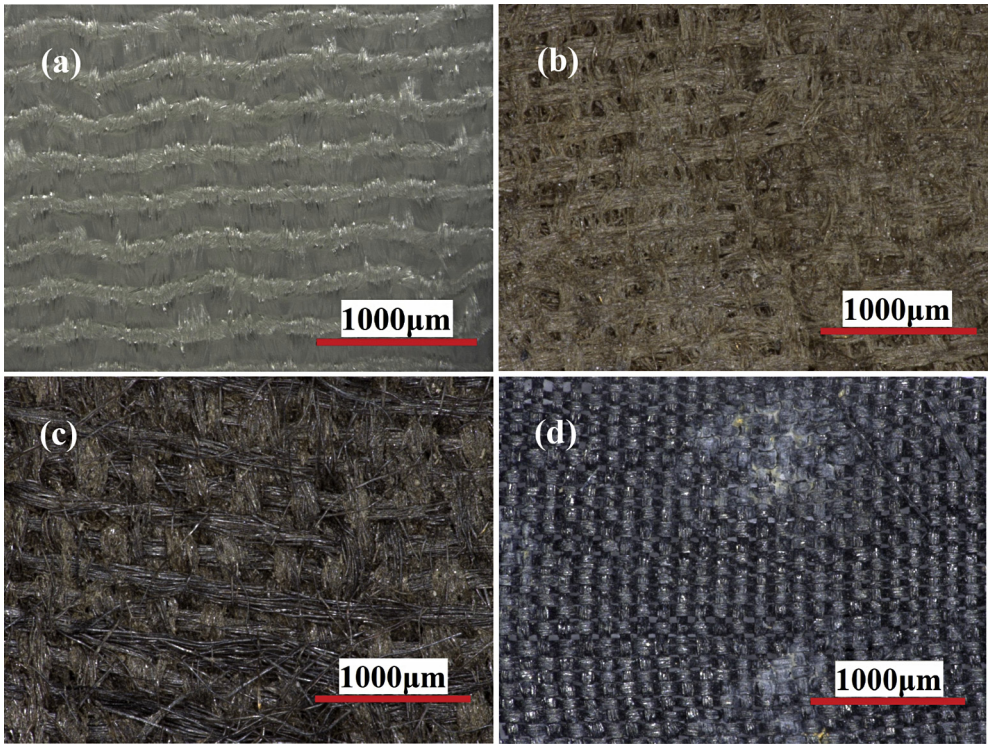

Fig. 1. Morphologies of the (a) modern control, (b) JZ, (c) LA and (d) YZ textile fragments.

Fig. 2. The data shows that spectra of the three ancient silk textiles have two resolved characteristic peaks at ~1360 cm^{-1} (termed ***D***) and ~1590 cm^{-1} (termed ***G***), which are absent in the control sample. The two peaks are the standard features of carbonization: peak ***D*** originating from the A_{1g} mode of a crystal lattice is induced by the particle size effect of small graphite crystals, and peak ***G*** originating from the E_{2g} species of the infinite crystal is a characteristic of the large single-crystal graphite [29]. The intensities of these two peaks increase monotonously in the spectra of the control, JZ, LA and YZ samples, implying the increasing degree of carbonization in the four silks. However, the Raman spectroscopy is inappropriate to study the carbonization behavior quantitatively via the signal amplitude due to the light dispersion and penetration.

3.3. The EPR spectroscopy analysis

The apparent morphological changes and Raman spectra in the four silk textiles indicate that the deterioration of the ancient samples is related to the carbonization of textiles during the long burial period. However, further in-depth information upon the carbonization process is not provided, namely, the kinetics of the carbonization. Therefore, EPR spectroscopy is employed and the results are shown in Fig. 3. All the EPR spectra have the same resolved characteristic absorption peak centered at the highly isotropic g-factor of 2.0037, indicating that the signals originate from the cubic symmetry of the radical center. Moreover, these single curves without hyperfine structure suggest that the spin density is localized at the atom(s) possessing the zero nuclear spin and the common stable paramagnetic metal species, *e.g.* Mn^{2+}, Cu^{2+} and Fe^{3+}, are excluded due to the peak-to-trough width (~1 mT) of the curves. Accordingly, the EPR spectra are assigned to that of the carbon radical. In addition, the unpaired electron is localized in the carbon radicals in the textile matrix according to the narrow peak-to-trough width and the slight asymmetry of the spectra [30]. Considering the identical sample weight, the concentrations of the radicals can be characterized by the signal intensity which is the weakest in JZ and the strongest in YZ in the three ancient silks. For the modern control sample, the intensity is close to the background noise level. The variation in concentration of the formed radicals is coincided with both the color change in Fig. 1 and the degree of carbonization shown in Fig. 2. Namely, the consecutive deterioration of the ancient silk textiles is concomitant with the accumulation of carbon radicals.

In order to clarify the formation kinetics of the radical, the cleavage of the peptide bonds in the silk fibroin is given in Fig. 4,

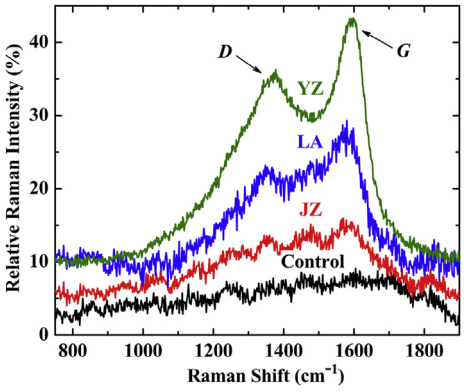

Fig. 2. Raman spectra of the modern control sample (Control), JZ, LA and YZ silk textiles, where the peaks ***D*** and ***G*** are indicated by arrows. Longitudinal shifts of 5%, 10% and 10% are performed for JZ, LA and YZ curves, respectively. The intensity of YZ sample is divided by a factor of 3 in order to fit with the other three ones.

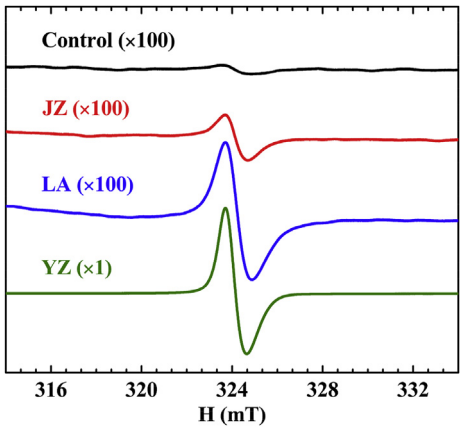

Fig. 3. EPR spectra of the modern control sample (Control) and three ancient silk textiles (JZ, LA and YZ).

where the three homolytic cleavage sites are indicated by ①, ② and ③, respectively. i) If a homolytic cleavage occurs at site ①, the hyperfine structures originating from the magnetic interaction between the spin of electron and nuclear will be observed due to the ^{14}N (nuclear spin I = 1) in the formed free radicals **1** and **2**. Thus it leads to three-band (2I+1 = 3) hyperfine structure, and the proton (1H, I = 1/2) ligated to the carbon radical center in the free radical **1** will complicate the hyperfine structure in the EPR spectrum. ii) In the case of site ②, an EPR spectrum without hyperfine structure will be detected originating from free radical **3**, while the radical **4**, a ^{14}N centered radical, is expected to have the resolved hyperfine structure from ^{1}H and ^{14}N. iii) At site ③, the radical **5** is also the ^{14}N centered radical similar to the radical **4** and the radical **6** has the hyperfine interaction with the direct ^{1}H ligand. It should be noted that other radicals, such as the oxygen-, nitrogen- and sulfur-centered radicals and the radical cations derived from saturated hydrocarbons, are highly reactive oxidizing species and short-lived in the ambient aerobic environment [31,32]. In summary, the homolytic cleavage of peptide bonds at the site ② is preferred in the case of a single step reaction, and the radical **3** will give rise to the EPR spectrum without hyperfine structure. Actually, silk degradation is a complicated process with various chemical bonds ruptured simultaneously [5,33]. However, only the stable carbon radical lasts and accumulates upon the long time history. A careful comparison was performed between the EPR signals of the

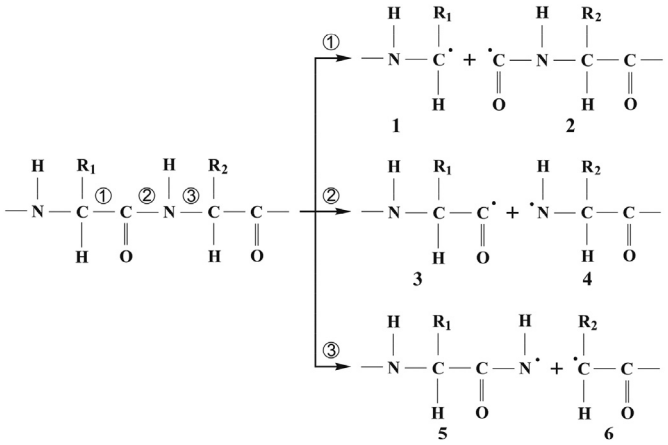

Fig. 4. Scheme of chemical structures of possibly formed radicals in ancient silk textiles. The corresponding three cleavage sites are denoted as ①, ② and ③.

ancient silk textiles and coal. The corresponding features herein, *i.e.* the highly isotropic g ~ 2.0037, the peak-to-trough width of ~1 mT and the slightly asymmetric spectral shape, are almost identical to those obtained from coal [34–36].

4. Conclusions

In summary, three ancient silk textiles of more than 2000 years were investigated and their degradation mechanism was discussed by means of Raman and EPR spectroscopy. The differences in color indicate that the degree of degradation of the JZ, LA and YZ samples are quite different due to the changed burial environments. Peaks ***D*** and ***G*** in the Raman spectra suggest that these ancient silk textiles have been carbonized. Furthermore, carbon free radicals were found using the EPR method. Basing on the absence of hyperfine structure, the peak-to-trough line width of ~1 mT and the slight asymmetry of the EPR spectra, the degradation of silk fibroin is a process of free radical chemistry. The present work may help achieve a better understanding of the degradation mechanism of silk textiles and thus contribute to the formulation of vigorous approaches to preserving valuable ancient silks.

Acknowledgments

We thank Prof. Jihu Su for helpful suggestions on the EPR discussions. Our thanks also go to the support from the Public Experimentation Center of University of Science and Technology of China (USTC). This work was financed by National Key Technology R&D Program (No. 2010BAK67B13) launched by the Ministry of Science and Technology of the People's Republic of China.

References

[1] Zhang YQ. Applications of natural silk protein sericin in biomaterials. Biotechnol Adv 2002;20(2):91–100.
[2] Mondal M, Trivedy K, Kumar SN. The silk proteins, sericin and fibroin in silkworm, Bombyx mori Linn., – a review. Caspian J Env Sci 2007;5(2):63–76.
[3] Dutta S, Bharali R, Devi R, Devi D. Purification and characterization of glue silk sericin protein from a wild silkworm antheraes assamensis helfer. Glob J Bio-Science & Biotechnol 2012;1(2):229–33.
[4] Miller JE, editor. A comparative analysis of degradation in naturally aged and experimentally degraded silk. Manhattan: Kansas State University; 1986.
[5] Zhang XM, Yuan SX. Measuring quantitatively the deterioration degree of ancient silk textiles by viscometry. Chin J Chem 2010;28(4):656–62.
[6] Baltova S, Vassileva V. Photochemical behaviour of natural silk–II. mechanism of fibroin photodestruction. Polym Degrad Stab 1998;60(1):61–5.
[7] Martel A, Burghammer M, Davies RJ, Riekel C. Thermal behavior of bombyx mori silk: evolution of crystalline parameters, molecular structure, and mechanical properties. Biomacromolecules 2007;8(11):3548–56.
[8] Numata K, Cebe P, Kaplan DL. Mechanism of enzymatic degradation of beta-sheet crystals. Biomaterials 2010;31(10):2926–33.
[9] Lu Q, Zhang B, Li MZ, Zuo BQ, Kaplan DL, Huang YL, et al. Degradation mechanism and control of silk fibroin. Biomacromolecules 2011;12(4):1080–6.
[10] Sen K, Babu KM. Studies on Indian silk. I. Macro characterization and analysis of amino acid composition. J Appl Polym Sci 2004;92(2):1080–97.
[11] Berghe IV. Towards an early warning system for oxidative degradation of protein fibres in historical tapestries by means of calibrated amino acid analysis. J Archaeol Sci 2012;39(5):1349–59.
[12] Garside P, Wyeth P, Zhang XM. Understanding the ageing behaviour of nineteenth and twentieth century tin-weighted silks. J Inst Conservat 2010;33(2):179–93.
[13] Sargunamani D, Selvakumar N. A study on the effects of ozone treatment on the properties of raw and degummed mulberry silk fabrics. Polym Degrad Stab 2006;91(11):2644–53.
[14] Shao JZ, Zheng ZH, Liu JQ, Carr CM. Fourier transform Raman and Fourier transform infrared spectroscopy studies of silk fibroin. J Appl Polym Sci 2005;96(6):1999–2004.
[15] Zhang XM, Wyeth P. Moisture sorption as a potential condition marker for historic silks: noninvasive determination by near-infrared spectroscopy. Appl Spectrosc 2007;61(2):218–22.
[16] Kavkler K, Gunde-Cimerman N, Zalar P, Demšar A. FTIR spectroscopy of biodegraded historical textiles. Polym Degrad Stab 2011;96(4):574–80.
[17] Greiff S, Kutzke H, Riekel C, Wyeth P, Lahlil S. Rob J, Paul W, editors. Scientific analysis of ancient and historic textiles. London: Archetype; 2004. p. 38.
[18] Hermes AC, Davies RJ, Greiff S, Kutzke H, Lahlil S, Wyeth P, et al. Characterizing the decay of ancient Chinese silk fabrics by microbeam synchrotron radiation diffraction. Biomacromolecules 2006;7(3):777–83.
[19] Brustolon M, Giamello E, editors. Electron paramagnetic resonance: a practitioner's toolkit. Hoboken: John Wiley & Sons, Inc; 2008.
[20] Yoshioka H, Koide N, Higashide F. ESR study of gamma-irradiated silk. Effect of oxygen. B Chem Soc Jpn 1974;47(10):2629–30.
[21] Liu RQ, Xie LL, Tu TC, Zu JH, Sheng KL. Properties of free radicals created by γ-ray irradiation of silk fabrics. Nucl Sci Tech 2002;02:110–4.
[22] Mamedov SV, Aktas B, Cantürka M, Aksakala B, Alekperova V, Bülbül F, et al. The ESR signals in silk fibroin and wool keratin under both the effect of UV-irradiation and without any external effects and the formation of free radicals. Biomaterials 2002;23(16):3405–12.
[23] Liu RQ, Xie LD, Sheng KL. ESR signals from silk fabrics irradiated by UV-rays. Nucl Sci Tech 2007;18(5):268–71.
[24] Luxford N, editor. Reducing the risk of open display: optimising the preventive conservation of historic silks. Southampton: University of Southampton; 2009.
[25] Koussoulou T. Photodegradation and photostabilization of historic silks in the museum environment – evaluation of a new conservation treatment. Papers from the Institute of Archaeology 10:75–88, doi:10.5334/pia.135.
[26] Khan MMR, Gotoh Y, Morikawa H, Miura M, Fujimori Y, Nagura M. Carbon fiber from natural biopolymer Bombyx mori silk fibroin with iodine treatment. Carbon 2007;45(5):1035–42.
[27] Khan MMR, Gotoh Y, Morikawa H, Miura M. Influence of iodine treatment on the carbonization behavior of Antheraea pernyi silk fibroin fiber. J Appl Polym Sci 2008;110(3):1358–65.
[28] Khan MMR, Gotoh Y, Morikawa H, Miura M. Graphitization behavior of iodine-treated Bombyx mori silk fibroin fiber. J Mater Sci 2009;44(16):4235–40.
[29] Tuinstra F, Koenig JL. Characterization of graphite fiber surfaces with Raman spectroscopy. J Compos Mater 1970;4:492–9.
[30] Mabbs FE, Collison D, editors. Electron paramagnetic resonance of d transition metal compounds. Michigan: Elsevier; 1992.
[31] Parsons AF. An introduction to free radical chemistry. Oxford: Wiley; 2000.
[32] Togo H. Advanced free radical reactions for organic synthesis. Chiba: Elsevier; 2003.
[33] Baltova S, Vassileva V, Valtcheva E. Photochemical behaviour of natural silk—I. Kinetic investigation of photoyellowing. Polym Degrad Stab 1998;60(1):53–60.
[34] Słowik GP, Więckowski AB. Paramagnetic centres in coal macerals. Acta Phys Pol A 2010;118(3):507–10.
[35] Kozdrowska L, Pilawa B, Więckowski AB. Influence of thermal decomposition on paramagnetic centres in vitrinite. Fuel Sci Technol Int 2004;85(14):1585–93.
[36] Plawa B, Więckowski AB. Groups of paramagnetic centres in coal samples with different carbon contents. Res Chem Intermed 2007;33(8):825–39.